NJC

Accepted Manuscript

This article can be cited before page numbers have been issued, to do this please use: Z. Liang, X. Wang, G. Dai, C. Ye, Y. Zhou and X. Tao, *New J. Chem.*, 2015, DOI: 10.1039/C5NJ01072A.

View Article Online
DOI: 10.1039/C5NJ01072A

Journal Name

ARTICLE

The solvatochromism and aggregation-induced enhanced emission based on triphenylamine-propenone

Received 00th January 20xx,
Accepted 00th January 20xx

DOI: 10.1039/x0xx00000x

www.rsc.org/

Zuo-Qin Liang,[a] Xiao-Mei Wang,[a,*] Guo-Liang Dai,[a] Chang-Qing Ye,[a] Yu-Yang Zhou,[a] Xu-Tang Tao[b]

Three new donor-π bridge-acceptor (D-π-A) compounds based on triphenylamine-propenone, namely 4-(1-phenylprop-2-en-1-one-3-yl)triphenylamine (PhO-TPA), 4-(1-(pyridin-2-yl)prop-2-en-1-one-3-yl)triphenylamine (PyO-TPA) and 4,4′,4″-(tri(1-(pyridin-2-yl)prop-2-en-1-one-3-yl))triphenylamine (TPyO-TPA), were synthesized through Aldol addition reaction. Their intramolecular charge transfer (ICT) and aggregation emission properties as well as packing structures were investigated. All of them show solvent polarity dependent emission. The density function theory calculations reveal that the ICT characteristic of the HOMO-LUMO transition is responsible for the large solvent effect. In aggregates, PhO-TPA and PyO-TPA exhibit aggregation-induced enhanced emission (AIEE). However, TPyO-TPA displays a different fluorescent behavior. Single-crystal analyses of PhO-TPA and PyO-TPA show that the weak intermolecular interactions and the suppression of the ICT state result in the efficient AIEE. The understanding on the AIEE fluorophores together with ICT characteristic will help to develop materials with color tenability, especially the ones with efficient emission in solid states.

Introduction

Conjugated organic materials with a D-π-A system, due to their unique photochemical and ICT properties,[1-3] have been the subject of active research and been widely applied in organic light-emitting diodes,[4-7] field-effect transisitors,[8-10] nonlinear optics,[11-13] photovoltaic devices,[14-16] biological fluorescent probes,[17-19] and so on. However, most of the D-π-A structured fluorophores generally suffer an aggregation-caused emission quenching process when fabricated into solid thin film, which greatly limits their applications, particularly in biophotonic and electroluminescent areas. A unique phenomenon termed as aggregation-induced emission (AIE) was observed by Tang's group with silole derivatives[20] and Park's group with CN-MBE nanopaticles[21]. Such molecules were nonemissive in solutions but exhibited intense emission once aggregated in concentrated solutions or casted pristine films. Attracted by the fascinating vistas, increasing attention has been paid to exploring new materials with AIE or AIEE characteristic and understanding the corresponding mechanism. To date, the AIE or AIEE effect caused by the restriction of intramolecular rotation[20,22-24] or specific molecular packing[21,25-27] has been effectively elucidated, including J-aggregation. Very recently, a new mechanism 'restricted ICT' was suggested by time-resolved fluorescence study of D-π-A structured cyano-substituted oligo (α-phenylenevinylene) (CNDPASDB).[28] Wang and co-workers examined the emission performance of CNDPASDB in different solvents and aggregate states. It displayed both remarkable solvatocromism and AIE. And the AIE properties significantly changed with solvent polarity. These new observations indicate that the previously verified mechanism of the restricted vibrational/torsional relaxation in the aggregation state is not complete in this case. Xu et al. reported a new D-π-A system OZA-SO, which also displayed AIE phenomenon by the restriction of ICT.[29] Besides, several materials with ICT and AIE properties were reported, for example, tetrabenzofluorene derivatives,[30] dicarbazolyl triphenylethylene derivatives.[31] The investigations on the D-π-A molecules may help to reveal the intrinsic process of the fluorescence enhancement and spectral shifts in their molecular aggregates.

As compared to inorganic materials, one of the prominent characteristics of organic materials is their structure flexibility. Subtle change in molecule structure can exert dramatic influence on the configuration, crystal stacking, electronic structure, and, furthermore, the optoelectronic property. The AIE/AIEE characteristic is caused in aggregation, so studying the relationship between the aggregate structures may be more important. In this work, three new D-π-A structured triphenylamine-propenone derivatives PhO-TPA, PyO-TPA and TPyO-TPA were synthesized by tuning the electron acceptor and the molecular shape. Their ICT and aggregation emission properties as well as packing structures were investigated. The fluorescence spectra of PhO-TPA, PyO-TPA and TPyO-TPA exhibit obvious solvatochromism. Their red-shifted emission

[a] Jiangsu Key Laboratory for Environment Functional Materials, School of Chemistry Biology and Material Engineering, Suzhou University of Science and Technology, Suzhou 215009, PR China. Tel: (+86)512-68326615; E-mail: wangxiaomei@mail.usts.edu.cn.
[b] State Key Laboratory of Crystal Materials, Shandong University, Jinan 250100, PR China.

Electronic Supplementary Information (ESI) available: Synthesis procedures, characterization, UV-visible absorption spectra in different polar solvents and in acetone/water mixtures with different volume fractions of water, and crystallographic data. See DOI: 10.1039/x0xx00000x

View Article Online
DOI: 10.1039/C5NJ01072A

and severely decreased quantum yield in polar solvents indicate that they have strong ICT characteristic. The Lippert-Mataga plots and electronic structures further prove it. Their emission intensity initially decreases with a low water fraction (f_w), due to the enhancement of the ICT effect. At a high f_w, they are in aggregates. PhO-TPA and PyO-TPA display AIEE characteristic, but TPyO-TPA is AIEE-inactive. Single-crystal analyses of PhO-TPA and PyO-TPA show that the weak intermolecular interactions and the suppression of the ICT state result in the efficient AIEE.

Results and discussion

Synthesis and characterization

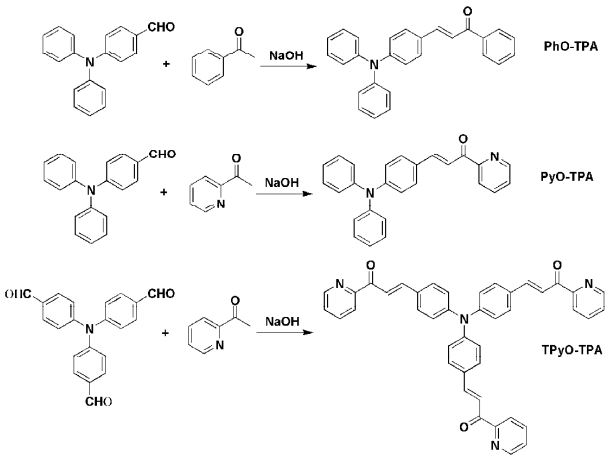

Scheme 1 Synthetic routes to the compounds.

The synthetic strategies and the structures of PhO-TPA, PyO-TPA and TPyO-TPA are depicted in Scheme 1. PhO-TPA was synthesized directly by Aldol addition reaction of acetophenone with 4-(diphenylamino)benzaldehyde in the presence of sodium hydroxide used as a catalyzer. The synthetic routes to obtain PyO-TPA and TPyO-TPA were almost the same as that of PhO-TPA, with the difference being in the use of the corresponding aldehyde and 2-acetylpyridine. These triphenylamine-propenone derivatives were verified by ^{1}H NMR, ^{13}C NMR and mass spectra. All of them are soluble in common organic solvents, such as toluene, tetrahydrofuran (THF), dichloromethane (DCM), acetone and N,N-dimethylformamide (DMF) but are insoluble in water. Single crystals of compounds PhO-TPA and PyO-TPA were prepared by a simple vapor diffusion method at room temperature and were characterized crystallographically.

Optical properties and ICT effect

Fig. 1 shows the normalized absorption spectra of three compounds in toluene (2.5×10^{-6} M). PhO-TPA demonstrates an absorption maximum at 358 nm. The absorption maximum of PyO-TPA and TPyO-TPA is located at 433 nm and 449 nm,

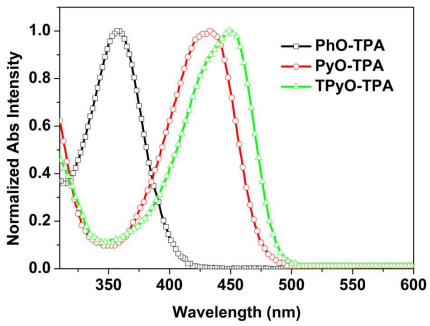

Fig. 1 Normalized UV-vis absorption spectra of PhO-TPA, PyO-TPA and TPyO-TPA in toluene (2.5×10^{-6} M).

respectively. The absorption maximum of PyO-TPA is red-shifted by 75 nm relative to that of PhO-TPA, due to PyO-TPA containing a stronger acceptor than PhO-TPA. Compared with compounds PhO-TPA and PyO-TPA, three-branched TPyO-TPA shows the greatest red-shift, which can be ascribed to its strong electron accepting ability and the extention of π-system. The photoluminescence (PL) spectra of three compounds in toluene (2.5×10^{-6} M) are shown in Fig. 2. PhO-TPA, PyO-TPA and TPyO-TPA show an emission maximum at 456 nm, 502 nm and 503 nm, respectively. All of the above information suggests that both absorption and PL spectra are in agreement with the order of the extension of the π-system and the increase of electron-accepting ability of the acceptor: acetylpyridine > acetophenone.

To get a clear investigation of ICT, the optical properties of PhO-TPA, PyO-TPA and TPyO-TPA in solvents of different polarity were investigated. When the solvent polarity changes from toluene to DMF, there are no significant changes in their absorption spectra (Fig. S1 in the Supporting Information). The corresponding absorption spectral data are summarized in Table 1. However, solvent polarity exerts a great effect on their PL emission, as shown in Fig. 2 and Table 1. With the increase of the solvent polarity, the PL spectrum of each compound is progressively shifted to a longer wavelength. The emission peaks of PhO-TPA, PyO-TPA and TPyO-TPA are 456, 502 and 503 nm in toluene and 535, 597 and 591 nm in DMF. Compared with the emission peak in toluene solution, the peak positions in DMF are red-shifted by 79, 95 and 88 nm for PhO-TPA, PyO-TPA and TPyO-TPA, respectively. Besides, PhO-TPA, PyO-TPA and TPyO-TPA show solvent polarity dependent emission Intensity. Three compounds have high emission in low polar solvents, but much lower emission in high polar solvents such as acetone and DMF. The PL quantum yields of three compounds in different polar solvents were measured by using an integrating sphere. The PL quantum yields of PhO-TPA, PyO-TPA and TPyO-TPA are 0.82, 0.59 and 0.81 in toluene, and 0.20, 0.05 and 0.04 in DMF, respectively. In toluene, the PL quantum yields are approximately 4-, 12-, and 20-fold higher as compared with those in DMF. The large bathochromic shift of PhO-TPA, PyO-TPA and TPyO-TPA combined with the decreased quantum yields should be

View Article Online
DOI: 10.1039/C5NJ01072A

related to the stabilization of the excited state. These behaviors are

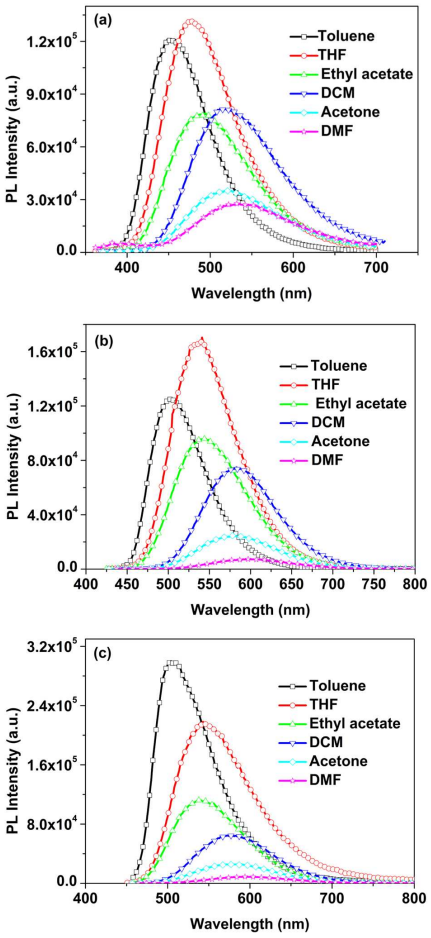

Fig. 2 PL spectra of PhO-TPA (a), PyO-TPA (b) and TPyO-TPA (c) in different polar solvents (2.5×10^{-6} M).

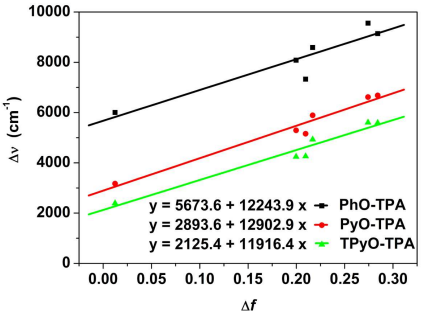

Fig. 3 Lippert-Mataga plots of PhO-TPA, PyO-TPA and TPyO-TPA in solvents of increasing polarity.

frequently observed in highly polarized molecules exhibiting enlarged dipoles and charge-transfer characteristics in their excited states.[1] The ICT state is known to be able to nonradiatively deactivate excited species, resulting in decreased quantum yield in polar solvents.[32] In order to further demonstrate the influence of solvent on fluorescence, the Lippert-Mataga plot of Stoke's shift (Δυ in cm^{-1}) against the orientation polarizability (Δf) was confirmed (Fig. 3). The

Table 1 Physical properties of PhO-TPA, PyO-TPA and TPyO-TPA in different polar solvents.

Cmpd		Toluene	THF	Ethyl acetate	DCM	Acetone	DMF
PhO-TPA	λ_{ab} [a]	358	354	351	359	352	354
	λ_{PL} [b]	456	478	490	519	523	535
	Φ [c]	0.82	0.89	0.63	0.67	0.25	0.20
	Δυ [d]	6003	7328	8082	8587	9141	9557
PyO-TPA	λ_{ab} [a]	433	423	423	434	418	428
	λ_{PL} [b]	502	541	545	583	580	597
	Φ [c]	0.59	0.85	0.55	0.42	0.12	0.05
	Δυ [d]	3174	5156	5292	5889	6682	6614
TPyO-TPA	λ_{ab} [a]	449	441	438	448	438	444
	λ_{PL} [b]	503	543	538	575	586	591
	Φ [c]	0.81	0.60	0.43	0.27	0.10	0.04
	Δυ [d]	2391	4260	4244	4930	5590	5602

[a] Peak position of the absorption maximum. [b] Peak position of PL, excited at the absorption maximum. [c] Quantum yields determined using an integrating sphere. [d] Stokes shift in cm^{-1}.

changes in Δυ with increasing solvent polarity are shown in Table 1. All of them exhibit a gradual increase in the Δυ upon increasing the polarity. The nice linear dependence of Δυ on Δf together with the large slope of the Δυ versus Δf plot further confirms that there are strong ICT behaviors in PhO-TPA, PyO-TPA and TPyO-TPA.

Electronic structures

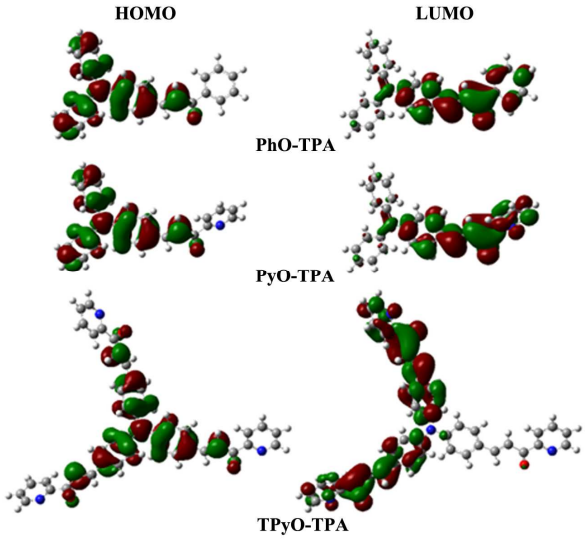

Fig. 4 Spatial distributions of the calculated HOMOs and LUMOs of PhO-TPA, PyO-TPA and TPyO-TPA.

View Article Online
DOI: 10.1039/C5NJ01072A

To better understand the photophysical properties of PhO-TPA, PyO-TPA, and TPyO-TPA, density function theory calculations were carried out by using the B3LYP/6-31G(d) level of theory embedded in the Gaussian 09 program.[33] The calculated electronic structures of the molecular orbits are shown in Fig. 4. All the molecules adopt twisted conformations. Such a twisted shape would hamper the tight π-π stacking interactions between the molecules, which would enable the fluorophores to emit efficiently in the condensed phase. The highest occupied molecular orbits (HOMO) of PhO-TPA, PyO-TPA and TPyO-TPA are mainly located on the electron-donating triphenylamine and bridged π units. The electron clouds of the lowest unoccupied molecular orbits (LUMO) for all the compounds are mainly located on the electron acceptors and its directly connected phenylvinyl groups. The near complete spatial separation between the HOMO and LUMO in PyO-TPA, PhO-TPA and TPyO-TPA indicates that substantial charge transfer from the donor moiety to the acceptor moiety when molecules are excited.

AIEE properties

To determine whether PhO-TPA, PyO-TPA and TPyO-TPA were AIEE-active or not, spectrometric verification tests were performed in various fractions of acetone/water mixtures. Water was used as a nonsolvent for three compounds in acetone. Concentration of the solution was kept at 2.0×10^{-5} M.

As shown in Fig. S2a in the Supporting Information, the absorption spectra of PhO-TPA are slightly affected, even if f_w increases up to 60%. When the f_w is further increased to 70%, the absorption spectrum is obviously red-shifted and exhibits Mie light scattering. At the same time, the absorption intensity dramatically drops. It demonstrates that molecules begin to aggregate in the solvent with this composition. The PL spectra of PhO-TPA in the acetone/water mixtures are shown in Fig. 5a. With the increase of the f_w from 0% to 60%, the PL intensity is gradually reduced and the emission peak is red-shifted from 530 nm to 549 nm. Because no obvious aggregates are observed, this change should be mainly attributed to the increase of solvent polarity. The interactions between polar solvent and solutes facilitate ICT effect. Increasing the f_w further, the PL intensity rises swiftly, accompanied by a blue-shift of the emission peak from 549 nm (f_w = 60%) to 498 nm (f_w = 90%). The increased PL intensity and blue-shifted emission peak may originate from the suppression of ICT effect. When f_w > 60%, PhO-TPA is in aggregated state. The hydrophobic environment is created inside the aggregates and the ICT excited state can't be stabilized. Therefore, the ICT effect is suppressed, and the dark state is eliminated. The relationship between the relative PL intensity (I/I_0) of PhO-TPA and the solvent composition of acetone/water mixtures is depicted in the inset of Fig. 5a. From the pure acetone solution to an acetone/water mixture with f_w = 80%, the PL intensity increases by 2.5-fold. So PhO-TPA is AIEE-active.

Similar effects are observed for PyO-TPA, as shown in Fig. 5b. With the increase of water content in acetone, the emission peak of PyO-TPA red-shifts first and then blue-shifts. In acetone PyO-TPA gives weak PL, and in an aqueous mixture with 90% water it emits a strong luminescence with a 3.4-fold increase in the I/I_0 ratio (Fig. 5b). Therefore, PyO-TPA also exhibits AIEE characteristic by the suppression of ICT effect.

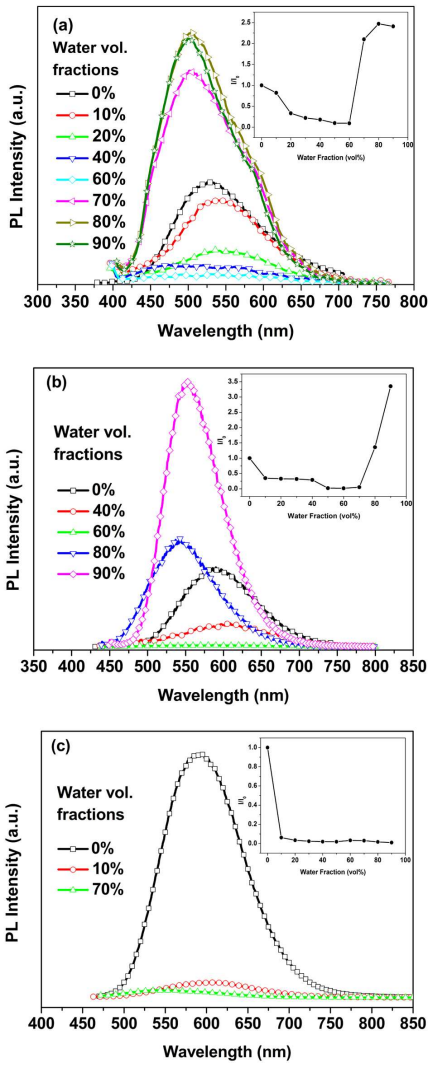

Fig. 5 PL spectra of PhO-TPA (a), PyO-TPA (b) and TPyO-TPA (c) (2.0×10^{-5} M) in acetone/water mixtures with different volume fractions of water. Insets: changes in the relative PL intensity (I/I_0) with the water fractions in acetone.

In contrast to the fluorescent behaviors of PhO-TPA and PyO-TPA, the emission intensity of TPyO-TPA shows a decreasing trend in aggregates (Fig. 5c). The pure acetone solution of TPyO-TPA has a relative intense fluorescence with an emission peak at 591 nm, which is dramatically quenched when a small amount of water (f_w = 10%) is added. Meanwhile, the emission peak is bathochromically shifted to 604 nm. This is a typical ICT effect arising from the increased solvent polarity. When more water (f_w > 50%) is added, the TPyO-TPA molecules forms aggregates (Fig. S2c in the Supporting Information). Although a hydrophobic environment is created inside the aggregates, the fluorescence does not recover. In the case of 90% volume

View Article Online
DOI: 10.1039/C5NJ01072A

fractions, the I/I_0 ratio is only 0.01. The different aggregation emission properties are thought to be related to the molecular structures.

Crystal structures

A different fluorescence behavior between PhO-TPA/PyO-TPA and TPyO-TPA (AIEE versus quenching) is obtained. To understand the relationship between optical properties and crystal structures, the crystal structures of PhO-TPA and PyO-TPA were determined by single crystal X-ray diffraction analysis. The important crystallographic data of PhO-TPA and PyO-TPA are listed in Table S1 in the Supporting Information.

Light yellow crystals of PhO-TPA were obtained by slow evaporation of a dichloromethane/ethanol mixture solution. The ORTEP diagram of PhO-TPA is shown in Fig. 6a. PhO-TPA adopts a twisted conformation in the crystals. The twist angle between the vinyl double bond (C8-C9) and the middle phenyl ring (C10-C15) is 14.7(6) °. In addition, the vinyl double bond and the terminal phenyl ring (C1-C6) don't lie in the same plane with a twist angle of 9.50(1) °. These twist angles and the propeller-shaped triphenylamine group can bring the steric hindrance effect to hinder the tight intermolecular packing. In the packing structure, the molecules are packed into molecular columns along the *a*-axis and the molecular columns are connected together by no classic hydrogen bond (C-H···O, I), as shown in Fig. 6b. For each molecular column, the molecules are connected together by the weak interactions C-H···O (II) and C-H···π (III) (Fig. 6c). Along the long and short axes of the molecular backbone, the twisted molecules adopt head-to-tail and slipped face-to-face packing, respectively. The shortest centroid to centroid distance between adjacent molecules is 4.53(2) Å (Fig. 6b). Thus, there is no typical intermolecular π-π interaction in the crystal of PhO-TPA. In addition, a triphenylamine group (donor group) is located far away from each acetophenone group (acceptor group). The shortest centroid to centroid distance between the donor group and the acceptor group is 4.80(7) Å (Fig. 6c). Therefore, an ICT excited state can't be stabilized in its crystal state.[34]

As for PyO-TPA, orange single crystals were prepared by vaporizing a petroleum solution. Its ORTEP diagram and packing arrangement in single crystal are given in Fig. 7. PyO-TPA also adopts a torsion conformation. The twist angles are 13.0(8) ° for the middle phenyl ring (C13-C18) and 9.28(2) ° for the pyridine group, relative to the vinyl double bond (C19-C20). The packing motif of PyO-TPA molecules is similar to that of PhO-TPA molecules. As shown in Fig. 7b, PyO-TPA molecules also pack into a column structure along the *a*-axis, due to the weak hydrogen bond (C-H···O, I) and van der Waals contacts (C···H, II and H···H, III). Within one column along the *a*-axis, it is arranged by the interactions C···H (IV), C-H···O (V) and C-H···π (VI) interactions (Fig. 6c). The key stacking forces of PhO-TPA are weak hydrogen bond and C-H···π interactions. Besides these two kinds of interactions, there are van der Waals interactions in the packing structures of PyO-TPA. And the distance of hydrogen bond and C-H···π interactions in PyO-TPA crystals is shorter than that of in PhO-TPA crystals. The intermolecular interactions of PyO-TPA are slightly stronger than those of PhO-TPA. Similarly, there is still no typical intermolecular π-π interaction and ICT excited state within the crystal structure of PyO-TPA. The shortest centroid to centroid distance between adjacent molecules is 4.55(7) Å, and that between the triphenylamine group (donor group) and the

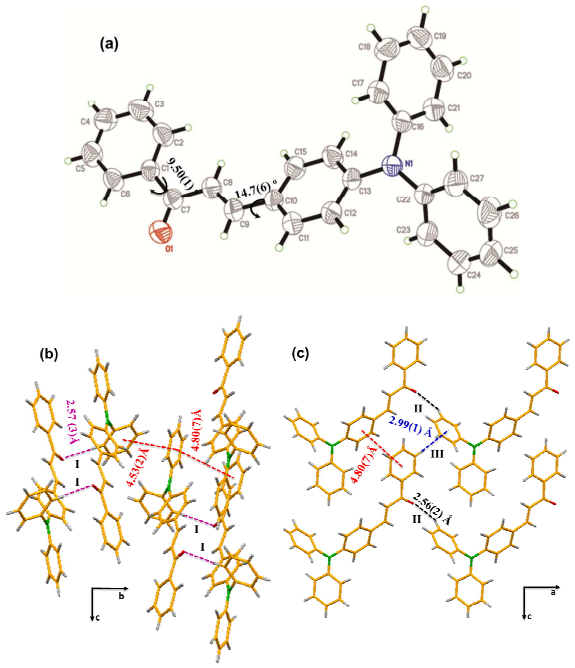

Fig. 6 (a) ORTEP diagram of PhO-TPA. (b) The interactions between adjacent molecules of PhO-TPA in the *bc* plane. The interaction for I is C17-H17···O1. (c) The interactions between adjacent molecules of PhO-TPA in the *ac* plane. The interaction for II is C18-H18···O1, and that for III is C5-H5···π (C16-C21).

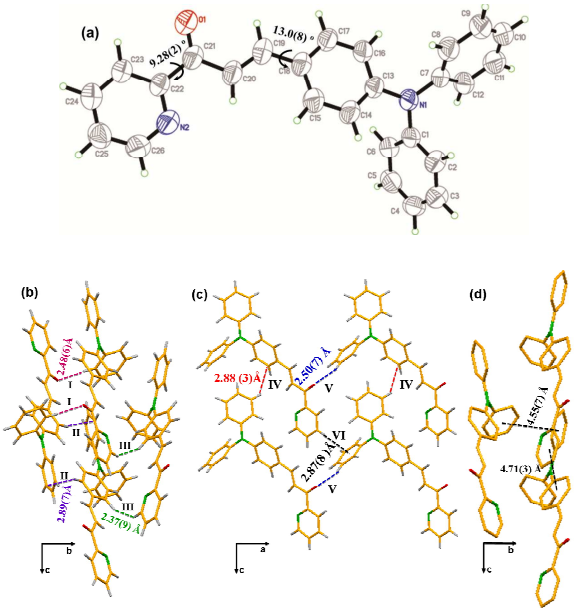

Fig. 7 (a) ORTEP diagram of PyO-TPA. (b) The interactions between adjacent molecules of PyO-TPA in the *bc* plane. The interaction for I is C6-H6···O1, that for II is C9···H17, and that for III is H15···H26. (c) The interactions between adjacent molecules of PyO-TPA in

View Article Online
DOI: 10.1039/C5NJ01072A

the *ac* plane. The interaction for IV is C15···H9, that for V is C5-H5···O1, and that for VI is C24-H24···π (C1-C6). (d) The centroid to centroid distance between adjacent molecules. The hydrogen atoms have been omitted for clarity.

acetylpyridine group (acceptor group) is 4.71(3) Å (Fig. 7d). The crystal of TPyO-TPA was not obtained. To better understand

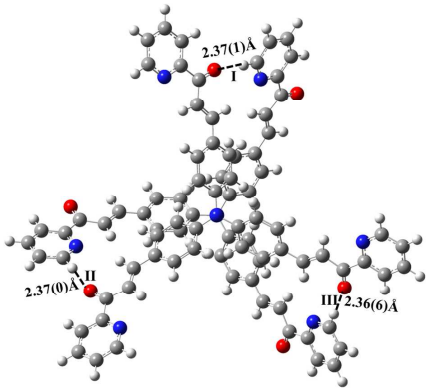

Fig. 8 The calculated packing structure and the C-H···O interactions of TPyO-TPA for dimer (a).

the relationship between the optical property and stacking mode of TPyO-TPA, the packing arrangements of its dimer, as the minimal supramolecular unit, were optimized by using the B3LYP/6-311+G** level. The optimized dimer configurations are shown in Fig. 8 for dimer (a) and in Fig S3 in the Supporting Information for dimer (b). The binding energies of two dimer configurations are 5.66 kcal/mol for (a) and 3.28 kcal/mol for (b). The packing structure of dimer (a) is stabler. In the packing structure of dimer (a), two molecules adopt face-to-face stacking mode. The stacking forces are the intermolecular C-H···O interaction, without intermolecular π-π interactions, as shown in Fig. 8. The interaction distance of three hydrogen bonds is about 2.37 Å, which is shortest in three compounds PhO-TPA, PyO-TPA and TPyO-TPA. In order to further analyze the intermolecular interactions, the geometry of dimer (a) obtained from B3LYP/6-311+G**was used to perform NBO analysis. In this packing structure, the origin of the interaction between two TPyO-TPA is the electron donation from the oxygen lone pair into the anti-bonding orbital of the C-H bond. The charge transfer energy $E^{(2)}$ are 2.32, 2.30 and 2.27 kcal/mol for hydrogen bond I, II and III, respectively. There are no significant interactions between other groups. Therefore, the ICT excited state can't also be stabilized in solid state. The weak fluorescence in aggregates may be ascribed to the intermolecular C-H···O interactions. The optimized geometry of TPyO-TPA lies on a threefold axis and has three identical substituents. These structural features should bring much more C-H···O packing forces than PyO-TPA in solid state. The multiple weak interactions often become significant, and play a significant role on the optical properties of materials.[35,36] In order to prove this interpretation, the PL properties of PyO-TPA and TPyO-TPA in solid state were investigated, as shown in Fig. 9. The powder of PyO-TPA emits at 560 nm, with a 58 nm red-shift in its emission maximum as compared to that in toluene. TPyO-TPA shows an emission maximum at 503 nm in toluene and at 601 nm in the powder. The longer red-shift is observed in the PL spectra of TPyO-TPA, which indicates that there are larger intermolecular interactions in the solid state.[37,38] The observation is in good agreement with our speculation.

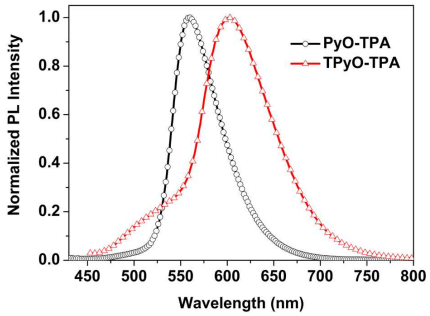

Fig. 9 Normalized PL spectra of PyO-TPA and TPyO-TPA in solid state.

Conclusions

Three donor-π bridge-acceptor structured triphenylamine-propenone derivatives have been synthesized, and their intramolecular charge transfer and aggregation emission properties as well as packing structures were investigated. All of them show solvent polarity dependent emission. The red-shifted emission spectra in polar solvents are attributed to the formation of intramolecular charge transfer state, which is able to nonradiatively deactivate excited species, and results in decreased quantum yield in polar solvents. In aggregates, PhO-TPA and PyO-TPA display AIEE characteristic, but TPyO-TPA is AIEE-inactive. Single-crystal analyses of PhO-TPA and PyO-TPA reveal that the weak intermolecular interactions and the suppression of the intramolecular charge transfer state lead to the emission enhancement in aggregates.

Acknowledgement

This work is supported by National Natural Science (Grant no. 51273141, 51303122, 21203135), Natural Science Foundation of Jiangsu Province (BK20130262), Natural Science Foundation of Education Department of Jiangsu Province (11KJA430003), Natural Science Foundation for colleges and universities in Jiangsu Province (14KJB150024), Excellent Innovation Team in Science and Technology of Education Department of Jiangsu Province, the Priority Academic Program Development of Education Department of Jiangsu Province (PAPD), Project of Science Technology of Suzhou (SYG201204), the Opening Project of Key Lab of Advanced Optical Manufacturing Technologies of Jiangsu Province (KJS1102) , the Youth Project of Suzhou University of Science and Technology (XKQ201312) and Collaborative Innovation Center of Technology and Material of Water Treatment.

View Article Online
DOI: 10.1039/C5NJ01072A

References

1 Z. R. Grabowski, K. Rotkiewicz, *Chem. Rev.*, 2003, **103**, 3899-4031.
2 Y. Zhu, S. Guang, X. Su, H. Xu, D. Xu, *Dyes and Pigments*, 2013, **97**, 175-183.
3 W. Z. Yuan, Y. Y. Gong, S. M. Chen, X. Y. Shen, J. W. Y. Lam, P. Lu, Y. W. Lu, Z. M. Wang, R. R. Hu, N. Xie, H. S. Kwok, Y. M. Zhang, J. Z. Sun, B. Z. Tang, *Chem. Mater.*, 2012, **24**, 1518-1528.
4 A. J. Heeger, *Chem. Soc. Rev.*, 2010, **39**, 2354-2371.
5 R. H. Friend, R. W. Gymer, A. B. Holmes, J. H. Burroughes, R. N. Marks, C. Taliani, D. D. Bradley, S. D. Dos, J. L. Bredas, M. Logdlund, W. R. Salaneck, *Nature*, 1999, **397**, 121-128.
6 Y. Shirota, *J. Mater. Chem.*, 2005, **15**, 75-93.
7 K. R. Justin Thomas, J. T. Lin, Y. T. Tao, C. H. Chuen, *Chem. Mater.*, 2004, **16**, 5437-5444.
8 T. Lei, Y. Cao, Y. L. Fan, C. J. Liu, S. C. Yuan, J. Pei, *J. Am. Chem. Soc.*, 2011, **133**, 6099-6101.
9 P. T. Wu, F. S. Kim, S. A. Jenekhe, *Chem. Mater.*, 2011, **23**, 4618-4624.
10 F. S. Kim, X. G. Guo, M. D. Watson, S. A. Jenekhe, *Adv. Mater.*, 2010, **22**, 478-482.
11 G. S. He, L. S. Tan, Q. Zheng, P. N. Prasad, *Chem. Rev.*, 2008, **108**, 1245-1330.
12 P. L. Wu, X. J. Feng, H. L. Tam, M. S. Wong, K. W. Cheah, *J. Am. Chem. Soc.*, 2009, **131**, 886-887.
13 P. Y. Gu, C. J. Lu, Z. J. Hu, N. J. Li, T. T. Zhao, Q. F. Xu, Q. H. Xu, J. D. Zhang, J. M. Lu, *J. Mater. Chem. C*, 2013, **1**, 2599-2606.
14 A. Mishra, C. Uhrich, E. Reinold, M. Pfeiffer, P. Bäuerle, *Adv. Energy Mater.*, 2011, **1**, 265-273.
15 H. X. Zhou, L. Q. Yang, S. C. Price, K. J. Knight, W. You, *Angew. Chem. Int. Ed.*, 2010, **49**, 7992-7995.
16 X. Zhang, J. W. Shim, S. P. Tiwari, Q. Zhang, J. E. Norton, P. T. Wu, S. Barlow, S. A. Jenekhe, B. Kippelen, J. L. Brédas S. R. Marder, *J. Mater. Chem.*, 2011, **21**, 4971-4982.
17 F. Qian, C. Zhang, Y. Zhang, W. He, X. Gao, P. Hu, Z. Guo, *J. Am. Chem. Soc.*, 2009, **131**, 1460-1468.
18 E. Kim, S. B. Park, *Chem. Asian J.*, 2009, **4**, 1646-1658.
19 E. Maçôas, G. Marcelo, S. Pinto, T. Cañeque, A. M. Cuadro, J. J. Vaquero, J. M. G. Martinho, *Chem. Commun.*, 2011, **47**, 7374-7376.
20 J. D. Luo, Z. L. Xie, J. W. Y. Lam, L. Cheng, H. Y. Chen, C. F. Qiu, H. S. Kwok, X. W. Zhan, Y. Q. Liu, D. B. Zhu, B. Z. Tang, *Chem. Commun.*, 2001, 1740-1741.
21 B.-K. An, S.-K. Kwon, S.-D. Jung, S. Y. Park, *J. Am. Chem. Soc.*, 2002, **124**, 14410-14415.
22 Y. Hong, J. W. Y. Lam, B. Z. Tang, *Chem. Soc. Rev.,* 2011, **40**, 5361-5388.
23 X. M. Wang, P. Yang, Q. F. Shi, W. L. Jiang, J. L.Chen, *Acta Chim. Sinica*, 2003, **61**, 1646-1652 (in Chinese).
24 K. Shiraishi, T. Kashiwabara, T. Sanji, M. Tanaka, *New J. Chem.*, 2009, **33**, 1680-1684.
25 Y. Liu, X. T. Tang, F. Z. Wang, J. H. Shi, J. L. Sun, W. T. Yu, Y. Ren, D. C. Zou, M. H. Jiang, *J. Phys. Chem. C*, 2007, **111**, 6544-6549.
26 C. J. Bhongale, C. W. Chang, C. S. Lee, E. W. G. Diau, C. S. Hsu, *J. Phys. Chem. B*, 2005, **109**, 13472-13482.
27 J. Clark, C. Silva, R. H. Friend, F. C. Spano, *Phys. Rev. Lett.*, 2007, **98**, 206406.
28 B. R. Gao, H. Y. Wang, Y. W. Hao, L. M. Fu, H. H. Fang, Y. Jiang, L. Wang, Q. D. Chen, H. Xia, L. Y. Pan, Y. G. Ma, H. B. Sun, *J. Phys. Chem. B*, 2010, **114**, 128-134.
29 P. Y. Gu, Y. H. Zhang, G. Y. Liu, J. F. Ge, Q. F. Xu, Q. Zhang, J. M. Lu, *Chem. Asian J.*, 2013, **8**, 2161-2166.
30 Y. Ueda, Y. Tanigawa, C. Kitamura, H. Ikeda, Y. Yoshimoto, M. Tanaka, K. Mizuno, H. Kurata, T. Kawase, *Chem. Asian J.*, 2013, **8**, 392-399.
31 H. Li, Z. Chi, B. Xu, X. Zhang, Z. Yang, X. Li, S. Liu, Y. Zhang, J. Xu, *J. Mater. Chem.*, 2010, **20**, 6103-6110.
32 S. Ji, J. Yang, Q. Yang, S. Liu, M. Chen, J. Zhao, *J. Org. Chem.*, 2009, **74**, 4855-4865.
33 M. J. Frisch, G. W. Trucks, H. B. Schlegel, et al., Gaussian 09, Revision A.02, Gaussian, Inc., Wallingford CT, 2009.
34 H. Tong, Y. Dong, M. Häußler, Y. Hong, J. W. Y. Lam, H. H-Y. Sung, I. D. Williams, H. S. Kwok, B. Z. Tang, *Chem. Phys. Lett.*, 2006, **428**, 326-330.
35 Z. Q. Liang, Y. X. Li, J. X. Yang, Y. Ren, X. T. Tao, *Tetrahedron Lett.*, 2011, **52**, 1329-1333.
36 Z. X. Wang, H. X. Shao, J. C. Ye, L. Zhang, P. Lu, *Adv. Funct. Mater.*, 2007, **17**, 253-263.
37 S. H. Ye, Y. Q. Liu, C. Di, H. X. Xi, W. P. Wu, Y. G. Wen, K. Lu, C. Y. Du, Y. Liu, G.Yu, *Chem. Mater.*, 2009, **21**, 1333-1342.
38 H. P. Zhao, F. Z. Wang, C. X. Yuan, X. T. Tao, J. L. Sun, D. C. Zou, M. H. Jiang, *Org. Electron.*, 2009, **10**, 925-931.

View Article Online
DOI: 10.1039/C5NJ01072A

A graphical and textual abstract for the contents pages

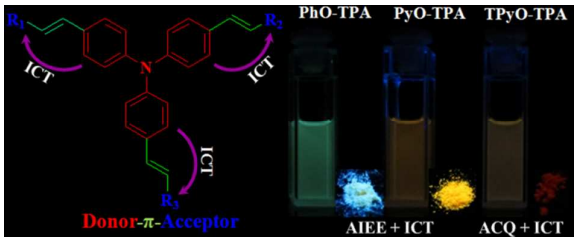

The weak intermolecular interactions and the suppression of the intramolecular charge transfer result in the efficient aggregation-induced enhanced emission characteristic of PhO-TPA and PyO-TPA.